

Flow-induced vibrations of long circular cylinders modeled by coupled nonlinear oscillators

GE Fei[†], LONG Xu, WANG Lei & HONG YouShi

State Key Laboratory of Nonlinear Mechanics, Institute of Mechanics, Chinese Academy of Sciences, Beijing 100190, China

The dynamics of long slender cylinders undergoing vortex-induced vibrations (VIV) is studied in this work. Long slender cylinders such as risers or tension legs are widely used in the field of ocean engineering. When the sea current flows past a cylinder, it will be excited due to vortex shedding. A three-dimensional time domain model is formulated to describe the response of the cylinder, in which the in-line (IL) and cross-flow (CF) deflections are coupled. The wake dynamics, including in-line and cross-flow vibrations, is represented using a pair of non-linear oscillators distributed along the cylinder. The wake oscillators are coupled to the dynamics of the long cylinder with the acceleration coupling term. A non-linear fluid force model is accounted for to reflect the relative motion of cylinder to current. The model is validated against the published data from a tank experiment with the free span riser. The comparisons show that some aspects due to VIV of long flexible cylinders can be reproduced by the proposed model, such as vibrating frequency, dominant mode number, occurrence and transition of the standing or traveling waves. In the case study, the simulations show that the IL curvature is not smaller than CF curvature, which indicates that both IL and CF vibrations are important for the structural fatigue damage.

vortex-induced vibration (VIV), vortex-induced wave (VIW), wake oscillator, long cylinder, fluid-structure interaction

Tensioned circular cylinders are widely used in offshore engineering. Observations of their response show vortex-induced vibration (VIV) to be a commonly occurring phenomenon, and VIV has the potential to cause costly fatigue failure. In the recent development of oil fields in deep waters, tension legs or risers with a large length-to-diameter aspect ratio are used. As the aspect ratio exceeds the order of 10^3 , cylinders undergo vortex-induced vibrations in high modes, and VIV may be one of the most important factors responsible for overall cylinder fatigue damage.

Attempts to quantify VIV have been made for decades, many of which are discussed in the comprehensive reviews of Sarpkaya^[1], Williamson et al.^[2,3] and Gabbai et al.^[4]. But with the wide usages of long cylinder in the last decade, more efforts have been made to conduct suitable experiments and establish advanced analysis tools for the assessment of long cylinder VIV. It is noted

that more attempts have been put on cylinder VIV in cross-flow (CF). The main reasons for less consideration of in-line (IL) vibrations are the lack of tests with combined IL and CF response, and that CF response was assumed to contribute far more to fatigue than IL. Some commercial codes used in offshore engineering, such as SHEAR7, VIVANA and VIVA, are developed to calculate structure VIV. However, they have some common shortcomings. The response is assumed to take place at a limited number of discrete frequencies and the programs are only able to calculate CF vibrations^[5]. Baarholm et al.^[6] indicated, however, that fatigue damage from IL vibrations may become significant for long cylinder

Received July 25, 2008; accepted November 10, 2008

doi: 10.1007/s11433-009-0128-8

[†]Corresponding author (email: gefei@imech.ac.cn)

Supported by the National Natural Science Foundation of China (Grant No. 10532070), the Knowledge Innovation Program of Chinese Academy of Sciences (Grant No. KJCX2-YW-L07), and the LNM Initial Funding for Young Investigators

structure. Therefore, the purpose of this research is to develop a model, following refs. [7–9], to calculate IL and CF response of the long tensioned cylinder.

There are two main methods for predicting the dynamic response of structure undergoing VIV. One method is the use of computational fluid dynamics (CFD), which consists of solving the Navier-Stokes (N-S) equation of fluid and the dynamic equation of a flexible cylinder. The two equations are coupled and the solving procedure is extremely computationally demanding. The alternative approach is to model the principle features of vortex shedding using a dynamical system instead of solving N-S equation. Facchinetti et al.^[8] verified the effect of cylinder movement on the lift fluctuation via different types of coupling terms (displacement, velocity and acceleration), which appears in a formulation of the wake oscillator model. Comparisons with experimental observations show that wake oscillator simulations were able to qualitatively and, in some point, quantitatively reproduce some aspects of VIV for rigid cylinders elastically supported and for flexible cylinders. Some parameters in the wake oscillator model, however, have to be derived from tests.

In our research, the wake oscillator model coupled with the cylinder dynamic equation has been extended to calculate the IL and CF response. The focus is on the case of the tensioned circular cylinder with a large aspect ratio subjected to uniform flow. Coupling between IL and CF vibration and structural geometric nonlinearity is accounted for. The comparisons with experimentally observed riser behavior from the test by Trim et al.^[10] have been made to verify the wake oscillator simulations.

1 Model formulation

A Cartesian right-hand coordinate system is defined with x and y in the horizontal plane and z vertically upwards. Considering a free-span circular cylinder with uniform material properties and constant diameter D , which follows the z -axis and is pinned at two ends (Figure 1), the dynamic equations can be expressed as

$$\begin{aligned} m \frac{\partial^2 x}{\partial t^2} + (C + C') \frac{\partial x}{\partial t} + EI \frac{\partial^4 x}{\partial z^4} - \frac{\partial}{\partial z} \left(T \frac{\partial x}{\partial z} \right) &= F_x, \\ m \frac{\partial^2 y}{\partial t^2} + (C + C') \frac{\partial y}{\partial t} + EI \frac{\partial^4 y}{\partial z^4} - \frac{\partial}{\partial z} \left(T \frac{\partial y}{\partial z} \right) &= F_y, \end{aligned} \quad (1)$$

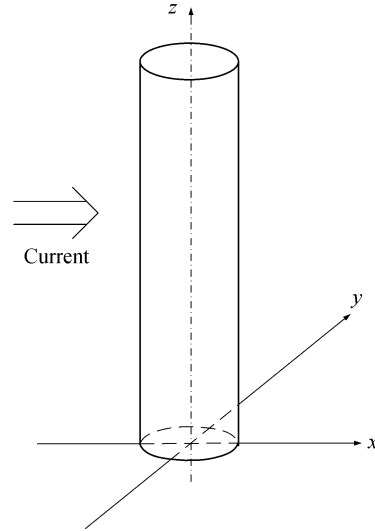


Figure 1 The sketch of the circular cylinder with a coordinate system.

where \bar{m} is the sum of structure mass m_s and added fluid mass m_f per unit length. Lacking a formulation of how m_f varies with cylinder deflection, then m_f is assumed independent of time, and \bar{m} is hence given by

$$\bar{m} = m_s + \frac{\pi}{4} C_a \rho D^2, \quad (2)$$

where C_a is the added mass coefficient, ρ is the fluid density, D is the cylinder diameter, C and C' are the damping coefficients due to structure and hydrodynamic forces. C' is related with vortex shedding frequency Ω_f and is given by

$$C' = \gamma \Omega_f \rho D^2, \quad (3)$$

where γ is a parameter determined through experiment. In eq. (1), EI is the bending stiffness of cylinder, and T is the axial tension in cylinder which can be expressed as

$$T = T_0 + EA \frac{S - L}{L}, \quad (4)$$

where L is the initial length, S is the length when the cylinder is deflected, T_0 is the initial tension force, E is Young's modulus of elasticity, A is the wall cross section area (stress area), and the prolongation $S - L$ of the cylinder due to the deflections is computed from

$$\frac{dS}{dz} = \sqrt{1 + \left(\frac{\partial x}{\partial z} \right)^2 + \left(\frac{\partial y}{\partial z} \right)^2}. \quad (5)$$

F_x and F_y in eq. (1) are the external hydrodynamic excitation forces due to the wake dynamics. Generally they can be considered as varying with the square of current speed, such that

$$F_x = \frac{1}{2} C_D \rho D U^2, \quad F_y = \frac{1}{2} C_L \rho D U^2. \quad (6)$$

Here, U is the current velocity acting normal to the cylinder. C_D and C_L are non-dimensional coefficients and represent the IL drag coefficient and CF lift coefficient, respectively. For a stationary cylinder, these coefficients are fairly well documented as a function of Reynolds number, but as the cylinder starts to oscillate the structure deflection will affect the fluid and therefore, the lift and drag coefficients. It has been found in experiment^[11] that the drag coefficient increases with increasing CF amplitude, and the drag coefficient will be expressed as

$$C_D = \bar{C}_D + \tilde{C}_D = C_{D0} \left(1 + K \frac{a_y}{D} \right) + C_{Di}, \quad (7)$$

where \bar{C}_D is the average drag coefficient, \tilde{C}_D is the pulsatory drag coefficient, C_{D0} is the drag coefficient for a cylinder at rest, K is a constant of magnitude 2, a_y is the amplitude of CF vibration and C_{Di} is a time varying vortex induced drag term. C_{Di} and C_L will be modeled by wake oscillator satisfying the van der Pol equation as done by Furnes et al.^[9]. To model C_{Di} and C_L , a set of non-dimensional variables q_x and q_y are introduced satisfying the following equations:

$$\frac{\partial^2 q_x}{\partial t^2} + \varepsilon_x \Omega_f (q_x^2 - 1) \frac{\partial q_x}{\partial t} + 4 \Omega_f^2 q_x = \frac{A_x}{D} \frac{\partial^2 x}{\partial t^2}, \quad (8)$$

$$\frac{\partial^2 q_y}{\partial t^2} + \varepsilon_y \Omega_f (q_y^2 - 1) \frac{\partial q_y}{\partial t} + \Omega_f^2 q_y = \frac{A_y}{D} \frac{\partial^2 y}{\partial t^2},$$

where q_x is the IL variable and q_y the CF variable. The vortex induced drag and lift coefficients are correspondingly modeled by

$$C_{Di} = C_{Di0} \frac{q_x}{2}, \quad C_L = C_{L0} \frac{q_y}{2}, \quad (9)$$

where C_{Di0} is the vortex shedding drag coefficient and C_{L0} is the lift coefficient for a fixed rigid cylinder subjected to vortex shedding. ε_x , ε_y , A_x , A_y in eq. (8) are non-dimensional parameters estimated through experiment. Ω_f is the Strouhal frequency given by

$$\Omega_f = 2\pi S_t \frac{U}{D}, \quad (10)$$

where S_t is the Strouhal number which is dependent

on the Reynolds number, and U is the current speed.

The right-hand sides of eq. (8) express the effects of cylinder motion on near wake. An acceleration coupling term is chosen as recommended by Facchinetti et al.^[8], which can quantitatively describe some typical phenomena of VIV observed experimentally to some extent.

For a cylinder at rest, the drag and lift forces coincide with the x - and y -axis, respectively, as shown in Figure 2(a). f_D is the average drag force acting on the cylinder, f'_D and f_L are the vortex induced drag and lift force, respectively. When the cylinder starts to vibrate as a result of vortex shedding, the drag and lift forces do not coincide with the x - and y -axis any more, which is shown in Figure 2(b). The corresponding forces exerted on the cylinder can thus be expressed as

$$F_x = f_D + f'_D \cos \theta - f_L \sin \theta, \quad (11)$$

$$F_y = f_L \cos \theta + f'_D \sin \theta,$$

where θ is the angle between the x -axis and the instantaneous velocity of the cylinder and is given by

$$\theta(t) = \arctg \left(\frac{\dot{y}(t)}{U - \dot{x}(t)} \right) = \arctg \left(\frac{\dot{Y}(t)}{1 - \dot{X}(t)} \right), \quad (12)$$

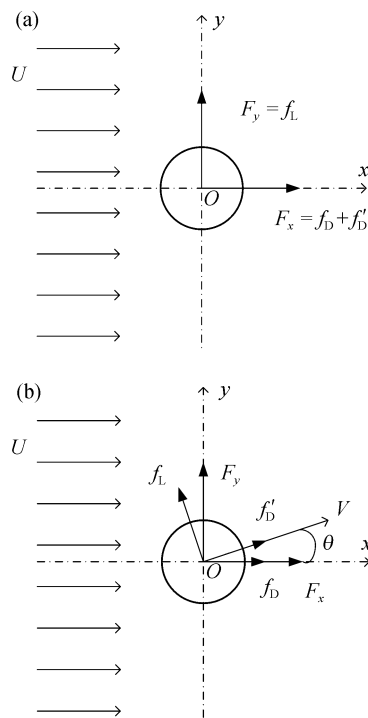


Figure 2 The illustration of the cross-section of the circular cylinder in a cross flow and the fluid forces exerted on it. (a) Stationary cylinder; (b) vibrating cylinder.

where the dot denotes differentiation with respect to time, $\dot{X}(t)$, $\dot{Y}(t)$ is the dimensionless velocity in the x and y direction, respectively. Since, in general, \dot{X} and \dot{Y} are smaller than 1, the angle θ is very small and

$$\begin{aligned}\sin \theta(t) &= \frac{\dot{Y}(t)}{\sqrt{\dot{Y}^2(t) + (1 - \dot{X}(t))^2}} \approx \dot{Y}(t), \\ \cos \theta(t) &= \frac{1 - \dot{X}(t)}{\sqrt{\dot{Y}^2(t) + (1 - \dot{X}(t))^2}} \approx 1.\end{aligned}\quad (13)$$

Substituting eq. (13) into (11), we get the formulation of the right-hand sides for eq. (1).

$$\begin{cases} F_x = f_D + f_D' - f_L \dot{Y}(t), \\ F_y = f_L + f_D' \dot{Y}(t). \end{cases}\quad (14)$$

2 Preliminary analysis of a tensioned cylinder

Axial tension T is assumed to be independent of z , which is based on that the variation of T along the cylinder axis is much smaller than the variation due to the cylinder deflection^[9,13]. eq. (1) then turns into

$$m \frac{\partial^2 \mathbf{r}}{\partial t^2} + (C + C') \frac{\partial \mathbf{r}}{\partial t} + EI \frac{\partial^4 \mathbf{r}}{\partial z^4} - T \frac{\partial^2 \mathbf{r}}{\partial z^2} = \mathbf{F}.\quad (15)$$

Here displacement vector is $\mathbf{r} = x + iy$, and hydrodynamic force vector is $\mathbf{F} = F_x + iF_y$. In the derivation of eq. (15), displacement vector \mathbf{r} is written as

$$\mathbf{r}(z, t) = \sum_{j=1}^n \phi_j(z) \bar{r}_j(t),\quad (16)$$

where $\phi_j(z)$ is the mode-shape function satisfying the cylinder boundary conditions. For a cylinder with pinned ends, the mode-shape function is hence given by

$$\phi_j(z) = \sin \frac{j\pi z}{L}, \quad j = 1, \dots, n,\quad (17)$$

where L is the length of cylinder. Substituting eqs. (16) and (17) into eq. (15) and using orthogonality of the mode-shape function, we have

$$\ddot{\bar{r}}_i + 2\zeta_i \omega_i \dot{\bar{r}}_i + \omega_i^2 \bar{r}_i = P_i(t).\quad (18)$$

Here,

$$\begin{aligned}\zeta_i &= \frac{C + C'}{2\bar{m}\omega_i}, \\ P_i(t) &= \frac{2}{\bar{m}L} \int_0^L F \sin \frac{i\pi z}{L} dz, \quad i = 1, \dots, n,\end{aligned}\quad (19)$$

where ω_i is the i th eigenfrequency of cylinder and can be expressed by

$$\omega_i = 2\pi f_i = \frac{i\pi}{L} \sqrt{\frac{EI}{\bar{m}} \left(\frac{i\pi}{L}\right)^2 + \frac{T}{\bar{m}}}.\quad (20)$$

3 Case study

The objective of this section is to verify if some aspects of the dynamics observed experimentally can be reproduced by the wake oscillator model described in sec. 2. Experiments on long riser ($L/D=1400$) were conducted at Marintek Ocean Basin in Trondheim and experimental data were published by Trim et al.^[10]. Figure 3 shows the plan view schematics of the test. The riser model has a mass ratio (ratio of riser mass to displaced fluid mass) of 1.6, and the length of 38 m. It is towed through the basin to generate desired current conditions. In the following, the current velocity is replaced by the towing speed, which was directly given in the test. Some detail characteristics of the riser are listed in Table 1. Water density is set as $\rho=1025 \text{ kg/m}^3$.

Although the Strouhal number is dependent on Reynolds number, it is here taken as constant, which is as-

Table 1 Riser characteristics

Riser diameter	Wall thickness
$D=0.027 \text{ m}$	$t_w=0.003 \text{ m}$
Length of the riser when not curved	Structure mass
$L=38 \text{ m}$	$m_s=0.939 \text{ kg/m}$
Young's modulus of elasticity	Axial tension
$E=36.2 \times 10^9 \text{ N/m}^2$	$T=4-6 \text{ kN}$

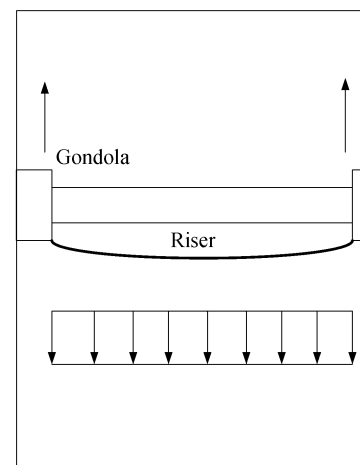


Figure 3 The plan view schematics of riser VIV testing^[10].

sumed to be an approximation for the subcritical range. For a cylinder undergoing vibration, the Strouhal number is set as 0.17. This value is lower than the usually quoted 0.2, but has been found to apply for moving cylinders^[12]. The added mass coefficient C_a is dependent on several variables like current speed and vibration amplitude. But since there is no efficient way of estimating the variations, it will be set as constant and for a cylinder C_a is taken a value of 1.0 as done by Furnes et al.^[9].

The drag coefficient for a cylinder at rest C_{D0} , the vortex shedding drag coefficient C_{Di0} and the vortex shedding lift coefficient C_{L0} all depend on Reynolds number. These are given as $C_{D0} = 1.2$, $C_{Di0} = 0.1$ and $C_{L0} = 0.3$ for a rigid cylinder at the subcritical range^[9]. Values for the coefficients in the wake oscillator equations (eq. (8)) were recommended by Facchinetti et al.^[8] as $\varepsilon_x = 0.3$, $\varepsilon_y = 0.3$, $A_x = 12$ and $A_y = 12$.

This system is numerically integrated in time and space using a standard centered finite differential method of the second order in both domains. The time step used in calculation is chosen much smaller than the critical time step and its effect on the results was checked. The initial conditions of the system are expressed as

$$r(z, 0) = 0, \quad \frac{\partial r(z, 0)}{\partial t} = 0, \quad (21)$$

$$q_x = q_y = 2, \quad \frac{\partial q_x}{\partial t} = \frac{\partial q_y}{\partial t} = 0. \quad (22)$$

Eq. (21) means that the initial conditions of zero displacement and velocity are applied to the riser. As for wake oscillator, it is assumed that the initial values of fluid variables are equal to 2.0, and the first derivatives with respect to time are set to zero.

Some features of riser dynamics can be illustrated by inspecting the eigenfrequencies and mode-shapes of a tensioned cylinder. The eigenfrequency as a function of mode number i for the riser model is shown in Figure 4. Values for a tensioned string and an untensioned beam with equal length L and mass per unit length m_s are also shown. The tensioned string and untensioned beam both have the pinned ends, which are the same with the riser. Therefore, the formulations of their eigenfrequencies are written as^[6]

$$\text{untensioned beam, } f_{i,\text{beam}} = \frac{i^2 \pi}{2} \sqrt{\frac{EI}{mL^4}},$$

$$\text{tensioned string, } f_{i,\text{string}} = \frac{i}{2} \sqrt{\frac{T}{mL^2}}. \quad (23)$$

The eigenfrequency of the riser model is seen to follow the tensioned string case for the lower modes, and then becomes closer to the untensioned beam case as the mode number increases. This means that the stiffness of the riser will be tension-dominated for the lower modes. The bending stiffness becomes increasingly important for the increasing of the mode order.

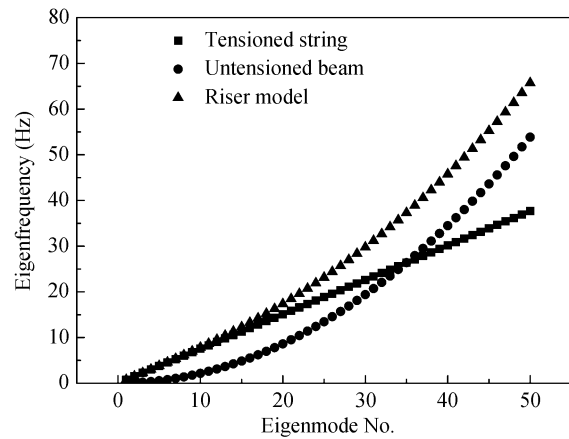


Figure 4 Estimates of eigenfrequency for riser, tensioned string and untensioned beam.

Figures 5 and 6 present the comparisons between relevant simulation results and experimental data, where the towing speed varies from 0.3 to 2.4 m/s with an increasing step of 0.1 m/s. Figure 5 shows how the riser frequency of CF and IL vibration varies with the towing speed. The lower straight line is the Strouhal frequency, based on the towing speed and a Strouhal number of 0.17, and the upper straight line represents the value twice the Strouhal frequency. For comparison, the experimental result^[10] is also drawn in Figure 5, and it is seen that the frequency of IL or CF vibration fits the Strouhal frequency if the towing speed is smaller than 1.4 m/s. As the towing speed increases, riser frequency starts to deviate from Strouhal frequency, but the frequency of IL vibration still remains twice the CF vibrating frequency. The result, computed by the wake oscillator model, indicates that the frequency for IL and CF vibration coincides well with the Strouhal frequency in all cases. As expected, both simulation and test results show that the frequency of riser vibration increases linearly with the towing speed.

Figure 6 shows the dominant mode number increases with the increasing of towing speed for both IL and CF

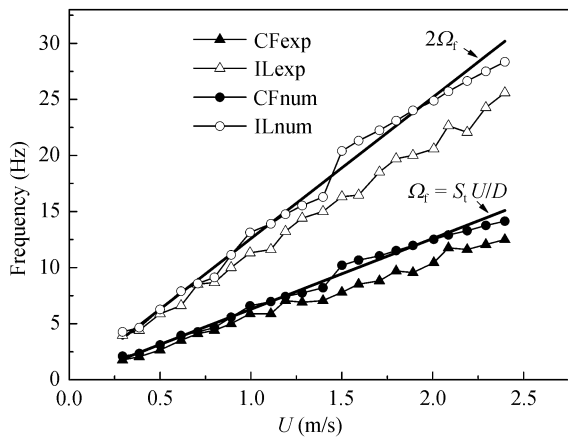


Figure 5 Frequency of riser vibration versus towing speed. Circular symbols represent simulation results and triangle symbols represent experimental data.

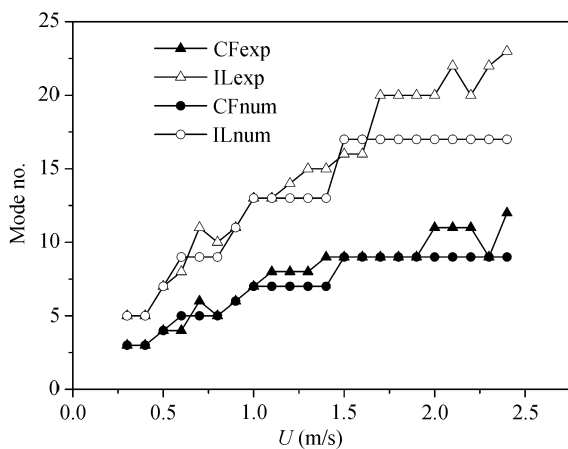


Figure 6 The dominant mode of riser vibration versus towing speed. Circular symbols represent simulation results and triangle symbols represent experimental data.

vibrations. The dominant mode number for CF vibration predicted by the wake oscillator model is seen to fairly fit the experimental result. But for IL vibration, good coincidence exists only when the towing speed is smaller than 1.6 m/s. However, for both simulation and test results, IL dominant mode number is approximately twice CF dominant mode number, and the mode number is always smaller than 25 in all cases. Referring to the riser model eigenfrequency presented in Figure 4, one observes that the eigenfrequency of the riser model is close to the tensioned string for the lower modes. It means that the eigenfrequency of the riser is sensitive to the variation of tension force for the lower modes. In the model testing, initial axial tension varies in a range from 4 to 6 kN, while in our calculation the initial tension within the riser is set to 5 kN. The tension difference between the test and calculation will possibly cause the

numerical result deviates from the experimental result as the towing speed increases. The same discrepancy is also reported by Kevin et al.^[13] using a CFD approach.

Figure 7 shows the average root mean square (r.m.s) of curvature for the riser model. For both IL and CF vibrations the average curvature increases approximately linearly with the towing speed. One observes that the IL curvature is not smaller than CF curvature. It indicates that the contribution to the riser fatigue damage from the IL vibration will be in the same order of magnitude as it from the CF vibration. The same conclusion is also reported in Baarholm et al.^[6] and Trim et al.^[10], where they found that the extent of IL vibration induced fatigue damage is similar to that caused by CF vibration. This conclusion is very important for engineering design because VIV analysis computer programs almost ignore the contribution of IL component to fatigue damage.

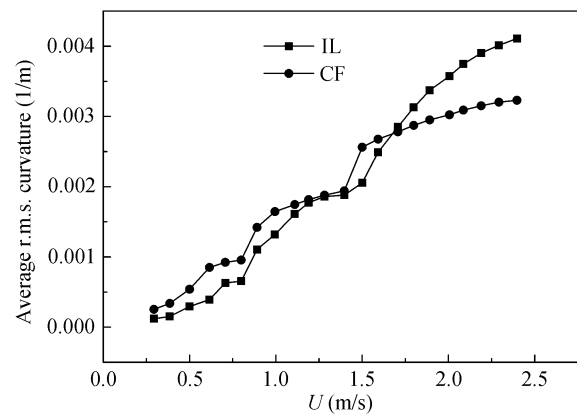


Figure 7 Average r.m.s. curvature of the riser versus towing speed. Square symbols represent the curvature in the IL direction and circular symbols represent the curvature in the CF direction.

Figures 8 and 9 show the time evolution of IL and CF displacements at every span position computed by the wake oscillator model. It is seen that the wake oscillator model predicts a combination of standing and traveling waves for the riser response. Standing waves dominate the response near the ends of the riser. In between the two end regions, traveling waves can be observed. The same dynamic behavior has been reproduced using DNS approach^[14] and model testing^[15]. Moreover, the occurrence of traveling waves would be affected by the towing speed. As shown in Figures 8 and 9, when the towing speed is equal to 1.5 m/s, standing waves dominate the riser response for both IL and CF. As the towing speed increases, traveling waves begin to occur and progressively dominate the response away from the riser

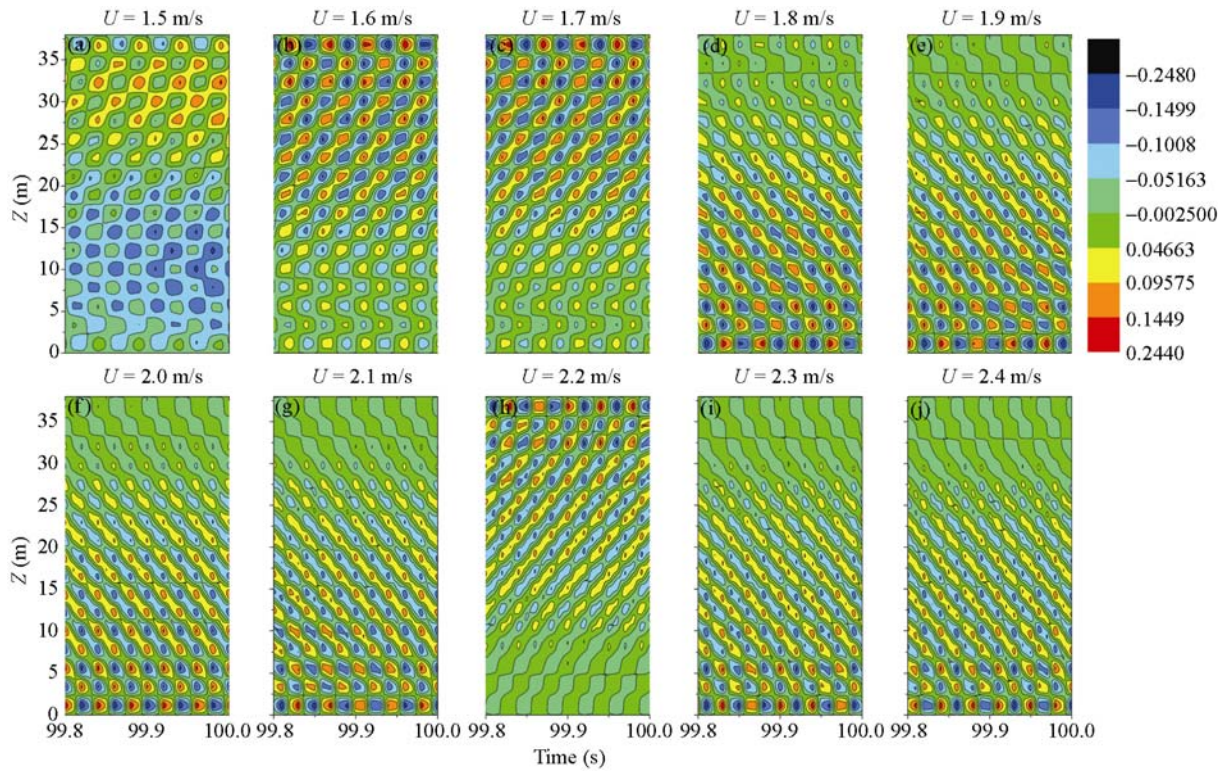


Figure 8 Evolution of IL displacement with time and space. In all figures the displacement level ranges from $-0.248D$ to $0.244D$ with equally spaced intervals.

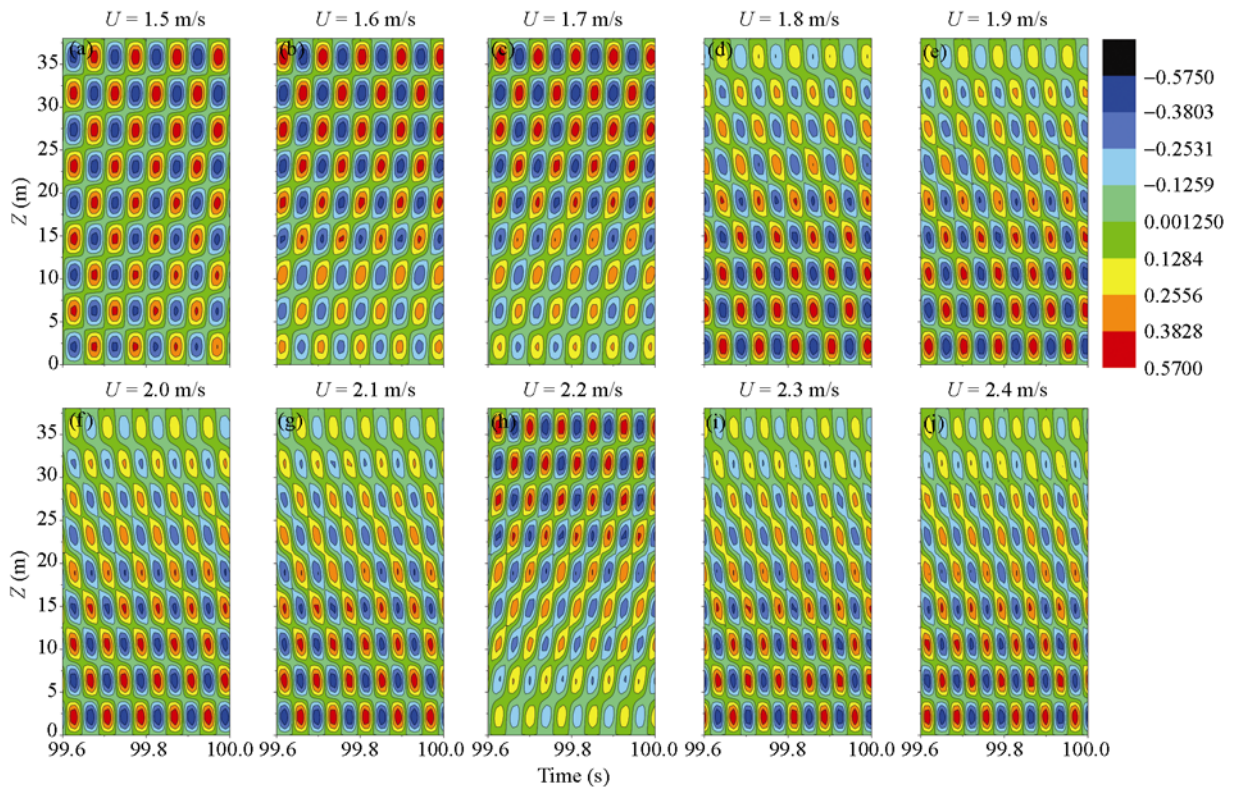


Figure 9 Evolution of CF displacement with time and space. In all figures the displacement level ranges from $-0.575D$ to $0.57D$ with equally spaced intervals.

ends. The occurrence of traveling waves inhibits the excitation of higher mode as the towing speed increases, which is also illustrated by Figure 6. The propagation direction of those traveling waves is arbitrary as reported by Violette et al.^[16].

4 Concluding remarks

A time domain model has been formulated to examine flow induced vibrations of long circular cylinders such as risers and tension legs. Current force describing the effects of wake on the cylinder vibration was formulated by a velocity-square-dependent model. This formulation contains the drag and lift coefficients that vary with time and are coupled with the cylinder motions itself. For the determination of these coefficients, a pair of non-linear oscillators located along the axial direction, including IL and CF vibrations, were introduced. The oscillators used are the classical van der Pol equations that simulate the wake dynamics. Coupling effect due to cylinder vibration on the wake oscillator is modeled by the acceleration of cylinder, and the parameters in wake oscillator

have been determined based on published experimental data. Moreover, this system introduced the coupling term between IL and CF fluid forces to reflect the relative motion of cylinder to current.

Because of the simplicity of the model, all the results presented in this paper require only a few hours of CPU time on a PC. This is one of the advantages of the present phenomenological approach over the CFD computations, and makes it possible to undertake large parametrical studies for VIV of long cylinders which are used in engineering applications.

A model validation versus the data from Marintek Ocean Basin with free span riser is presented. It is shown that some important dynamics features of long cylinders undergoing VIV can be modeled using a simple wake oscillator approach. These features include vibrating frequency, vibrating mode number, response curvature, transition of the standing and traveling waves. The simulations also show that the IL curvature is not smaller than CF curvature, which indicates that both IL and CF vibrations are important for the structural fatigue damage.

- 1 Sarpkaya T. A critical review of the intrinsic nature of vortex-induced vibrations. *J Fluids Struct*, 2004, 19: 389–447
- 2 Williamson C H K, Govardhan R. Vortex-induced vibrations. *Annu Rev Fluid Mech*, 2004: 413–455
- 3 Williamson C H K, Govardhan R. A brief review of recent results in vortex-induced vibrations. *J Wind Eng Ind Aerodyn*, 2008, 96: 713–735
- 4 Gabbai R D, Benaroya H. An review of modeling and experiments of vortex-induced vibration of circular cylinders. *J Sound Vib*, 2005, 282: 575–616
- 5 Chaplin J R, Bearman P W, Cheng Y, et al. Blind predictions of laboratory measurements of vortex-induced vibrations of a tension riser. *J Fluids Struct*, 2005, 21: 25–40
- 6 Baarholm G S, Larsen C M, Lie H. On fatigue damage accumulation from in-line and cross-flow vortex-induced vibrations on risers. *J Fluids Struct*, 2006, 22: 109–127
- 7 Wang X Q, So R M C, Chan K T. A non-linear fluid force model for vortex-induced vibration of an elastic cylinder. *J Sound Vib*, 2003, 260: 287–305
- 8 Facchinetti M L, de Langre E, Biolley F. Coupling of structure and wake oscillator in vortex-induced vibrations. *J Fluids Struct*, 2004, 19: 123–140
- 9 Furnes G K, Sorensen K. Flow induced vibrations modeled by coupled non-linear oscillators. In: Chung J S, Hong S W, Nagata S, et al., eds. *Proceedings of the 17th International Offshore and Polar Engineering Conference*, Lisbon, Portugal. California: ISOPE, 2007. 2781–2787
- 10 Trim A D, Braaten H, Lie H, et al. Experimental investigation of vortex-induced vibration of long marine risers. *J Fluids Struct*, 2005, 21: 335–361
- 11 Sarpkaya T. Fluid forces on oscillating cylinders. *J Waterw Port Coast Ocean Eng-ASCE*, 1978, 104: 275–290
- 12 Lie H, Kaasen K E. Modal analysis of measurements from a large-scale VIV model test of a riser in linearly sheared flow. *J Fluids Struct*, 2006, 22: 557–575
- 13 Kevin H, Chen H C. Riser VIV analysis by a CFD approach. In: Chung J S, Hong S W, Nagata S, et al., eds. *Proceedings of the 17th International Offshore and Polar Engineering Conference*, Lisbon, Portugal. California: ISOPE, 2007. 2722–2729
- 14 Newman D J, Karniadakis G E. A direct numerical simulation study of flow past a freely vibrating cable. *J Fluid Mech*, 1997, 344: 95–136
- 15 Facchinetti M L, de Langre E, Biolley F. Vortex-induced travelling waves along a cable. *Eur J Mech B-Fluids*, 2004, 23: 199–208
- 16 Violette R, de Langer E, Szydlowski J. Computation of vortex-induced vibrations of long structures using a wake oscillator model: Comparison with DNS and experiments. *Comp Struct*, 2007, 85: 1134–1141